applied sciences

MDPI

Article

Reinforcement Design of the Support Frame of a Petrochemical Heater

Chun-Lang Yeh

Department of Aeronautical Engineering, National Formosa University, Huwei, Yunlin 632, Taiwan; clyeh@nfu.edu.tw; Tel.: +886-5631-5527

Abstract: In this paper, we investigated the operating security of the support frame of a petrochemical heater under the action of a strong wind. When the fatigue limit was exceeded, the support frame was damaged. We monitored the heater before reinforcement and then applied the finite element method to analyze and compare nine different kinds of reinforcement methods for the support frame. From the results of the finite element analysis, fatigue failure of the support frame before reinforcement occurred at locations where the computed stresses from the finite element analysis were large, thus partially justifying the adequacies of the present analysis methods and results. Among the nine reinforcement methods, we suggest case 9 to reinforce a support frame so that its operating security under the action of a strong wind can be improved. At the end of this paper, several future studies are suggested, including verification of the reinforcement for the support frame and the establishment of the system for automatic stress monitoring and analysis.

Keywords: heater; support frame; vibration; stress analysis

Citation: Yeh, C.-L. Reinforcement Design of the Support Frame of a Petrochemical Heater. *Appl. Sci.* **2022**, *12*, 5107. https://doi.org/10.3390/app12105107

Academic Editors: Alberto Campagnolo and Alberto Sapora

Received: 18 April 2022
Accepted: 16 May 2022
Published: 19 May 2022

1. Introduction

The petrochemical facilities comprise a storage tank, reactor, heater, tower, separator, pipeline, rotating machinery, etc., among which the heater is the major source of energy and steam. A heater is a kind of heavy energy consumption equipment whose performance and operating security are closely connected with the profits, capacities, and product qualities of the petrochemical industry. Owing to the demand of environmental protection and greenhouse gas reduction, the improvement and maintenance of heaters as well as the reduction and prevention of pollutions are undoubtedly tasks that have high return on investment (ROI) and instant results.

A typical petrochemical heater comprises a convection section, radiation section, waste heat recovery system, burners, support frames, and the ventilation system. Huang, et al. [1], investigated the dynamic response of a stack to an earthquake at a nearby site. They summarized the results of a response spectrum analysis of two stacks, including the Tupras stack and a generic U. S. stack. They also used a demand-collapse comparison to present a nonlinear static analysis of the collapsed stack. The results confirmed that the stack could readily fail under the considered earthquake and were also consistent with the debris pattern. Mojtaba Haratian, et al. [2], developed a mathematical model associated with genetic algorithms. The model took the operational and geometric constraints into account. It was used to design the convection section, radiant chamber, stack section, and other subsections of a heater, with the aim to optimize the total annual cost. The authors declared that the proposed model could yield an economically/realistically optimal design up to 2.48% cheaper than the original design. Guo, et al. [3], discussed the strengthening measures and weak points of a natural gas heater in detail. The authors proposed two effective optimizing arrangements of the heat exchange surfaces to enhance the heat transfer: (a) thermally retarding and cooling the heated surface, and (b) setting baffles among the heating surfaces. It was found that the energy consumption was reduced and

the thermal efficiency of the heater was improved. Mohd Nazarudin Rosli and Norashid Aziz [4] reviewed two methods of calculating the overall heat transfer coefficient (U) in steady state modelling of a steam cracking furnace radiant section using Aspen PLUS. They evaluated and compared some U values to find the optimal U for their proposed model. They found that the U value of 165 $W/m^2 \cdot K$ gave the best estimate for the industrial data. Liu [5] combined the experimental study and finite element simulation to design different tube structures for the requirements of different high temperatures, including Co-C 1324 °C, Pt-C 1738 °C, and Re-C 2474 °C. The main research topics included (1) the study of the precise measurement method for the axial temperature profiles of a furnace tube and (2) the methods of tube structure improvement using software simulation and experimental methods. The author compared different curves of axial temperature distribution to determine the optimal structure of the tube. Experiments were used to verify the simulation results. Jiang, et al. [6], used stick multi-degree-of-freedom models to numerically analyze the response of tall, reinforced concrete (RC) chimneys under an earthquake. The effects of eccentricity for two RC chimneys (150 m and 210 m tall) were studied. They also studied the seismic stresses and influences of the vertical ground motion for the two chimneys. Numerical results revealed that by considering existing eccentricities, the tensile and compressive stresses of the two chimneys might increase under the actions of some specific earthquake waves. Scarabino and Bacchi [7] numerically analyzed the flow within and outside of a chimney that had a low length–to-diameter ratio and a lateral inlet for combustion gases. They discussed the dispersion of gases in the atmosphere and the problematic flow configuration detected. They also proposed a flow straightener to reduce the vorticity within the chimney. Numerical results revealed that the flow straightener proposed could reduce the streamlines' deviation from 35–40° to less than 5°.

From the above literature related to heaters, it can be seen that in addition to experimental measurements, the numerical simulation (e.g., finite element method (FEM)) has also been used successfully to analyze vibrations and stresses of the structure. Several relevant studies using numerical simulation to analyze vibrations and stresses of the structure are reviewed below. Naresh Reddy Kolanu, et al. [8], proposed a unified and generic numerical modeling approach for stiffened carbon fiber-reinforced polymer (CFRP) panels considering both the intra- and inter-laminar damage modes. A progressive damage model (PDM) based on the 3D finite element method was proposed to simulate the collapse behavior of a single blade-stiffened composite CFRP panel under uniaxial compression loading. The authors validated the developed PDM by comparing the stability response, collapse load results, damage evolution, failure mechanisms, ultimate load, and the displacement data with the experimental observations and estimates. Armentani, et al. [9], applied a multibody calculation method to analyze the vibration of a turbocharged diesel engine. They considered different modeling assumptions and simulated the angular speed variation of a crankshaft. Moreover, they performed time dependent simulation of the engine supports and compared with experimental results. They also used a multibody model created with the AVL/EXCITE software to do the modal analysis, considering the damping aspects. Finally, they evaluated the influence of crankshaft torsional frequencies on the rotational speed behavior to reduce the vibration phenomena. In a later study [10], Armentani, et al., adopted a reduced modelling strategy to reduce the full FEM model size of the engine. The strategy was based on the component mode synthesis and was found to reduce the required runtime significantly.

Vibration-induced failure and lifetime assessment are also important in structure analysis. Several relevant studies are reviewed below. Leta, et al. [11], analyzed the lifetimes of fired heater tubes. The authors statistically characterized the uncertainty associated with the omega creep procedure of the API-579 Part 10 by treating the primary input parameters as random variables and processes. They also employed Monte Carlo simulations to estimate the probability of tubes failing for a specified time. Jaganathan Swaminathan, et al. [12], analyzed reformer catalyst tubes which had failed after eight years of service. They assessed the tube lifetime by the Larson–Miller parameter method. The authors

concluded that the failure was caused by local overheat, leading to premature creep failure. Ray, et al. [13], investigated the remaining life of the catalyst tubes of a fertilizer plant. The investigation included microscopy, hardness measurement, dimensional measurement, hot tensile tests, and accelerated creep tests. The authors concluded that overheating was the primary cause of the significant degradation in the microstructures and mechanical properties of the catalyst tubes. Giannella [14] reported a stochastic approach under variability of different input parameters to investigate the fatigue crack growth in a railway axle. They used the approach to predict the probability distribution of the residual fatigue life for a railway axle in the presence of defects when considering multiple sources of uncertainty. Matta and Szasz [15] discussed the vibration and fatigue failures at pipeline facilities. They reviewed the vibration phenomena occurring at pipeline facilities and took practical examples to illustrate the types and ways of resolving vibration-induced fatigue failures at pipeline facilities. Harper [16] investigated the damages caused by acoustic-induced vibrations and flow-induced vibrations in pipelines, plants, and facilities. He gave practical examples to illustrate the types and ways of resolving the two vibration-induced failures. Lennart G. Jansson, et al. [17], theoretically and experimentally discussed the piping vibration phenomena and the ways of preventing vibration-related damage. They also investigated an empirical rule by experimental measurement and numerical analysis. More literature related to vibration-induced failure and lifetime assessment can be found in the author's previous studies [18–20].

From the above literature, many experimental and numerical investigations in structure analysis have been conducted. However, very few structural analyses of petrochemical heaters were presented in public literatures. Nevertheless, the structural design of a heater is undoubtedly closely connected with its performance and operating security, which in turn strongly affects the profits, capacities, and product qualities of the petrochemical industry. Therefore, this study aims to investigate the operating security of a petrochemical heater under the action of a strong wind. When the fatigue limit was exceeded, the support frame was damaged. The support frames were made of steel and were used to bear the heater under the action of wind and gravity. In this study, we first performed an in situ measurement for the stress distribution of a petrochemical heater. Next, we applied the finite element method to analyze its vibration modes and stress distribution. The aims of this study were to ensure that (1) the potential threat of fatigue failure could be detected in an earlier phase, (2) the stress monitoring in situ, service life assessment, and subsequent improvement tasks could proceed smoothly, and (3) the operating security of the heater could be ensured.

2. Methodology

In this study, the heater was first monitored before reinforcement, in situ, to acquire the data required for stress analysis. A high-speed data acquisition recorder, strain gauge, anemorumbometer, and triaxial accelerometer were used to measure and record the strain, wind speed, wind direction, and acceleration at selected positions. The measured data were used for the subsequent stress analysis. We used SOLIDWORKS 2020 [21] to establish the numerical model of the heater. ANSYS Workbench 2020 [22] was then employed for stress analysis.

Structure analysis has been widely used in the design of structure. According to the nature of mechanics, structure analysis can be classified as static analysis and dynamic analysis. The latter includes modal analysis and harmonic response analysis. In structure design, static analysis is usually used to evaluate the displacement, strain, and stress of the structure due to inertial forces, e.g., gravity, centrifugal force, etc. Modal analysis is one of the methods of structure dynamic analysis. Mode is an intrinsic vibration characteristic of a linear system. Each mode has its own specifically intrinsic vibration frequency, form, and damping ratio. Harmonic response analysis can be used to analyze the response of the structure to the time-variant harmonic wave. Through the solution of frequency domain, the frequency response of the structure to harmonic wave loadings can be obtained to

examine if the system can alleviate the resonance, fatigue, or other harmful effects. The solutions of the equations for static and dynamic analyses of a structure can be found in books of structural engineering and mechanics, e.g., [23–25].

3. Vibration Measurement and Analysis

In this study, we first monitored the support frame and stack of a petrochemical heater before reinforcement, in situ. The heater was 62 m high. The stack of the heater was 47 m long, and its average diameter was 1.35 m. The steel grade of the heater was ASTM A36. We measured the strains of the support frame and stack at selected positions, as shown in Figure 1. These monitoring positions were determined by stress analysis for the original heater shown in Figure 2b using ANSYS.

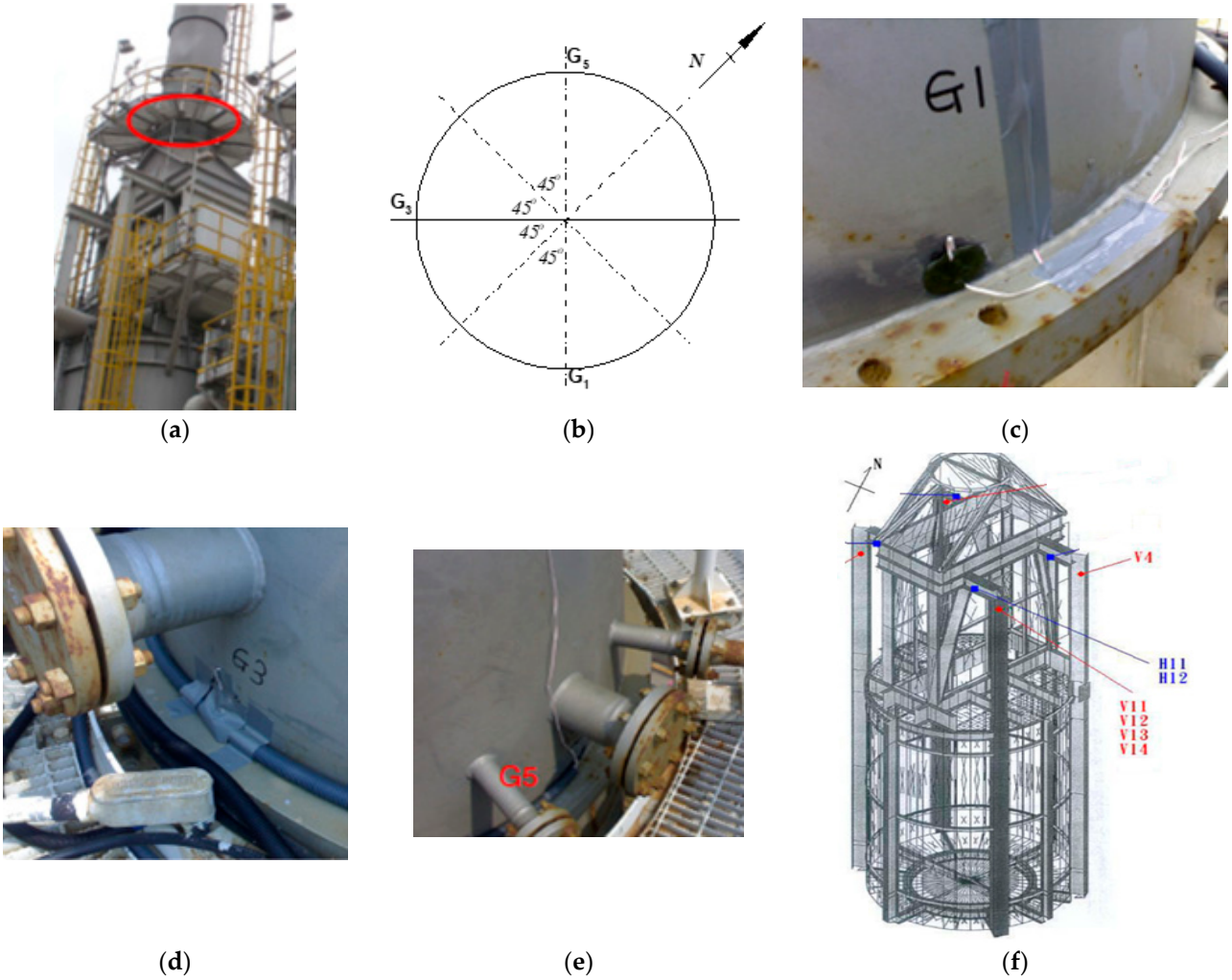

Figure 1. *Cont.*

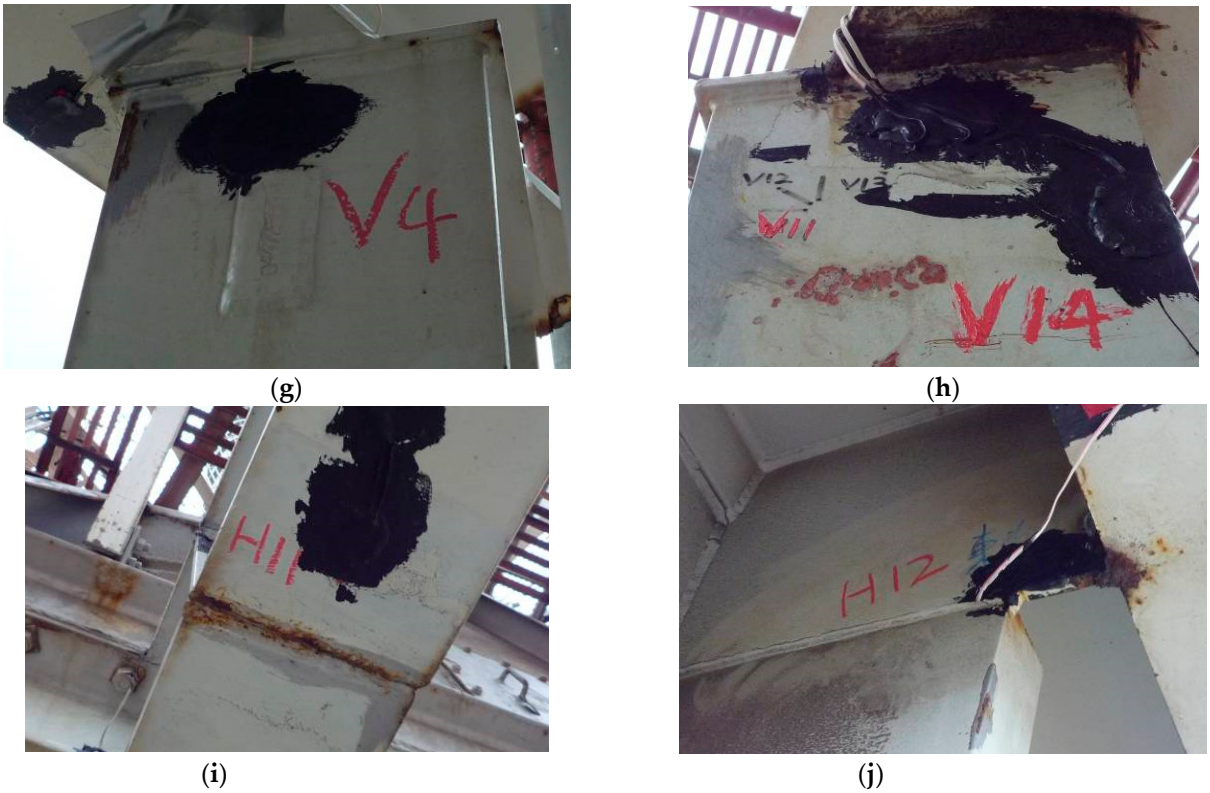

(**g**) (**h**)

(**i**) (**j**)

Figure 1. Stress-monitoring positions for the support frame and stack of a petrochemical heater before reinforcement: (**a**) Stress-monitoring positions of the stack (marked by red ellipse); (**b**) Orientation of the stress-monitoring positions of the stack; (**c**) Position G1; (**d**) Position G3; (**e**) Position G5; (**f**) Stress-monitoring positions of the support frame; (**g**) Position V4; (**h**) Position V14; (**i**) Position H11; (**j**) Position H12.

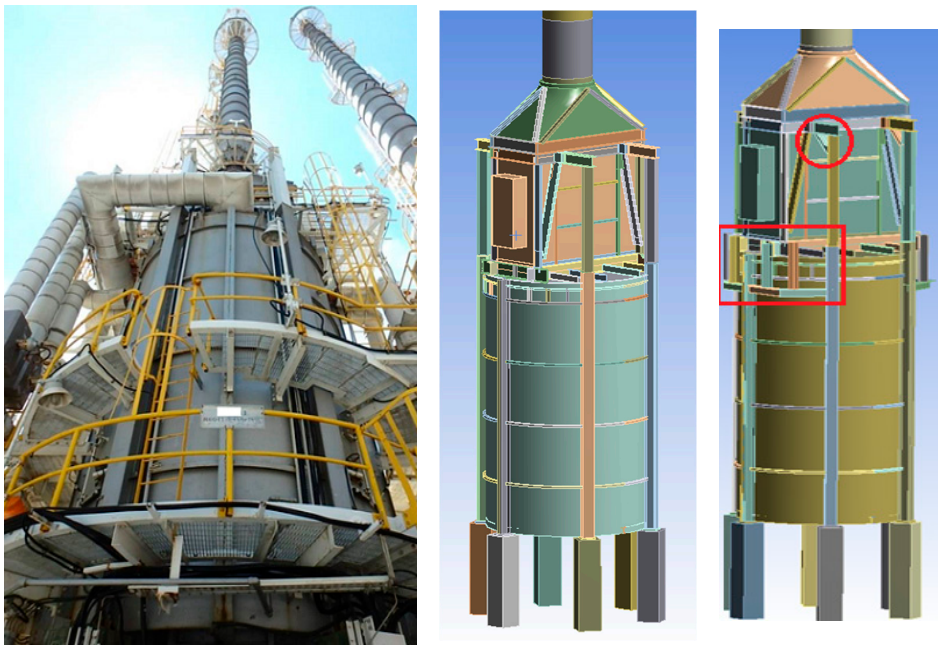

(**a**) (**b**) (**c**)

Figure 2. In Situ photograph and model of the heater. (**a**) in situ photograph, (**b**) model of original heater, (**c**) model of present heater (with reinforcement marked by circle and rectangle).

From the monitoring results, it was found that the stress of the stack did not exceed the fatigue limit (10.87 ksi or 75 MPa). However, the maximum stress amplitude at location V14 on the support frame was 14.3 ksi (or 98.6 MPa, consistent with 497.2754 μ strain, as shown in Figure 3), which exceeded the fatigue limit.

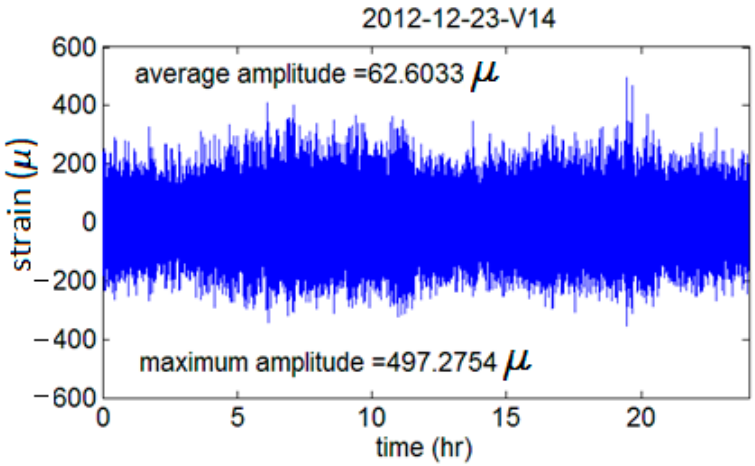

Figure 3. Measured strain at location V14 on the support frame.

In the following section, the finite element method was applied to analyze the stress distribution of the heater. We attempted to exert a force in the resonant vibration (northwest/southeast) direction on the heater until the stress at location V14 on the support frame reached 14.3 ksi (or 98.6 MPa). This force was then applied on both the heater before reinforcement and the heater with reinforced support frame. The results were analyzed and compared, and improvement suggestions for the support frame are proposed according to the analysis results so that the operating security of the heater can be improved.

4. Reinforcement and Stress Analysis of the Support Frame

In this study, we used SOLIDWORKS 2020 to establish the numerical model of the heater, as shown in Figure 2. The number of mesh elements for the numerical model was around 6×10^5, which was adequate for obtaining mesh-independent solution. The stress positions are illustrated in Figure 4. For the heater before reinforcement, whose model is shown in Figure 2b, the results of finite element analysis revealed that the stresses at positions 1–8, 9, 10, 14, 15, 17–19, 23, and 31–38, as shown in Figure 5, were in potential threat because the stresses exceeded or were close to the fatigue limit. Because fatigue failure of the support frame before reinforcement had occurred at positions 10 and 18, as shown in Figure 6, the results of the finite element analysis partially justified the adequacies of the present analysis methods. To improve the security of the heater before reinforcement, the heater was reinforced by adding braces, as marked in Figure 2c. The finite element analysis revealed that the stresses were significantly improved, but those at positions 1, 4, 10, and 31–38 still exceeded the fatigue limit, as shown in Figure 7.

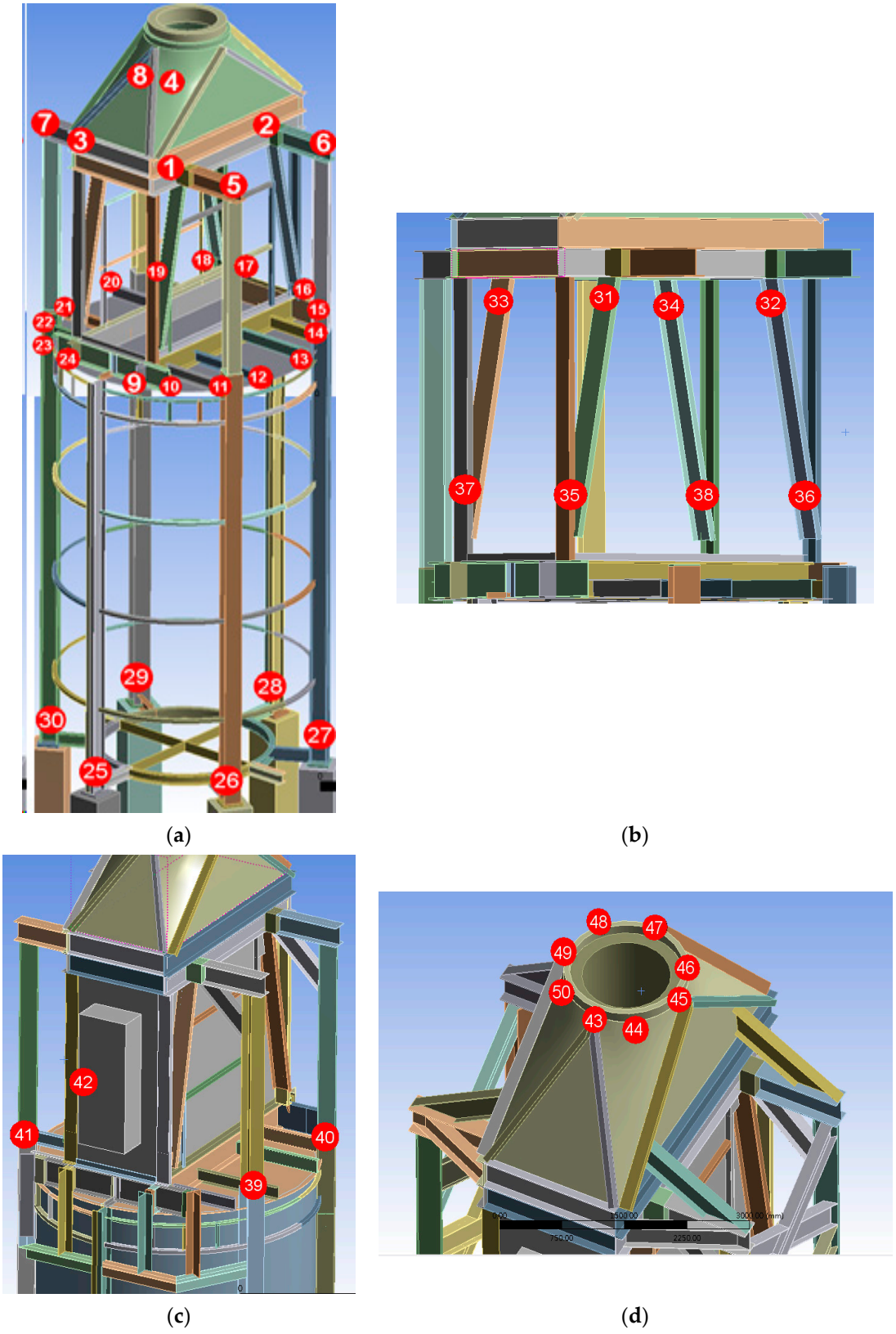

Figure 4. Illustration of the stress positions: (**a**) at the convection and radiation sections; (**b**) at the braces of the convection section; (**c**) at the junctions of the longitudinal beams; (**d**) near the root of the stack.

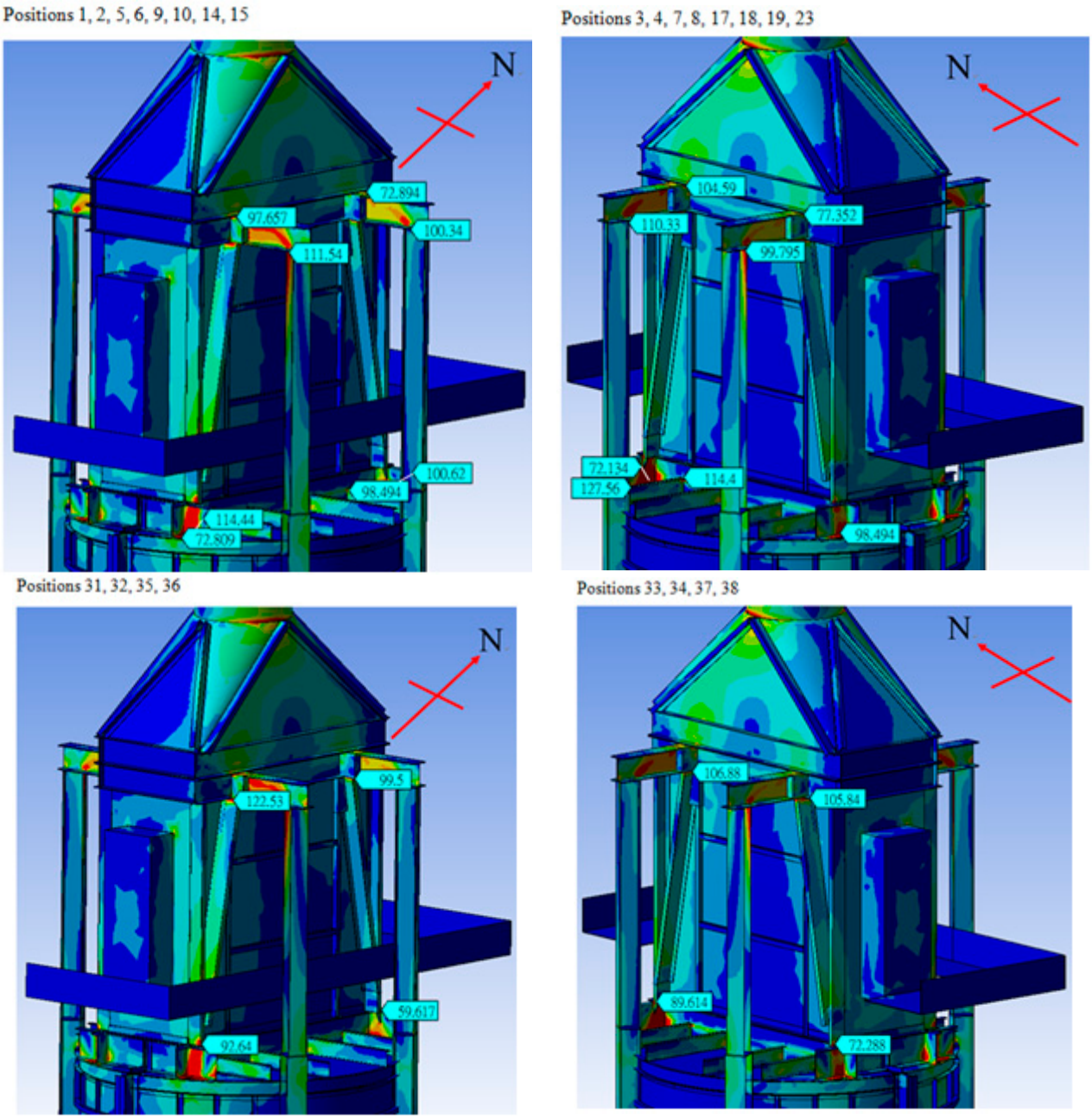

Figure 5. Results of finite element analysis for the heater before reinforcement.

(**a**) (**b**)

Figure 6. Fatigue failure of the support frame before reinforcement: (**a**) at the south-east side; (**b**) at the north-west side.

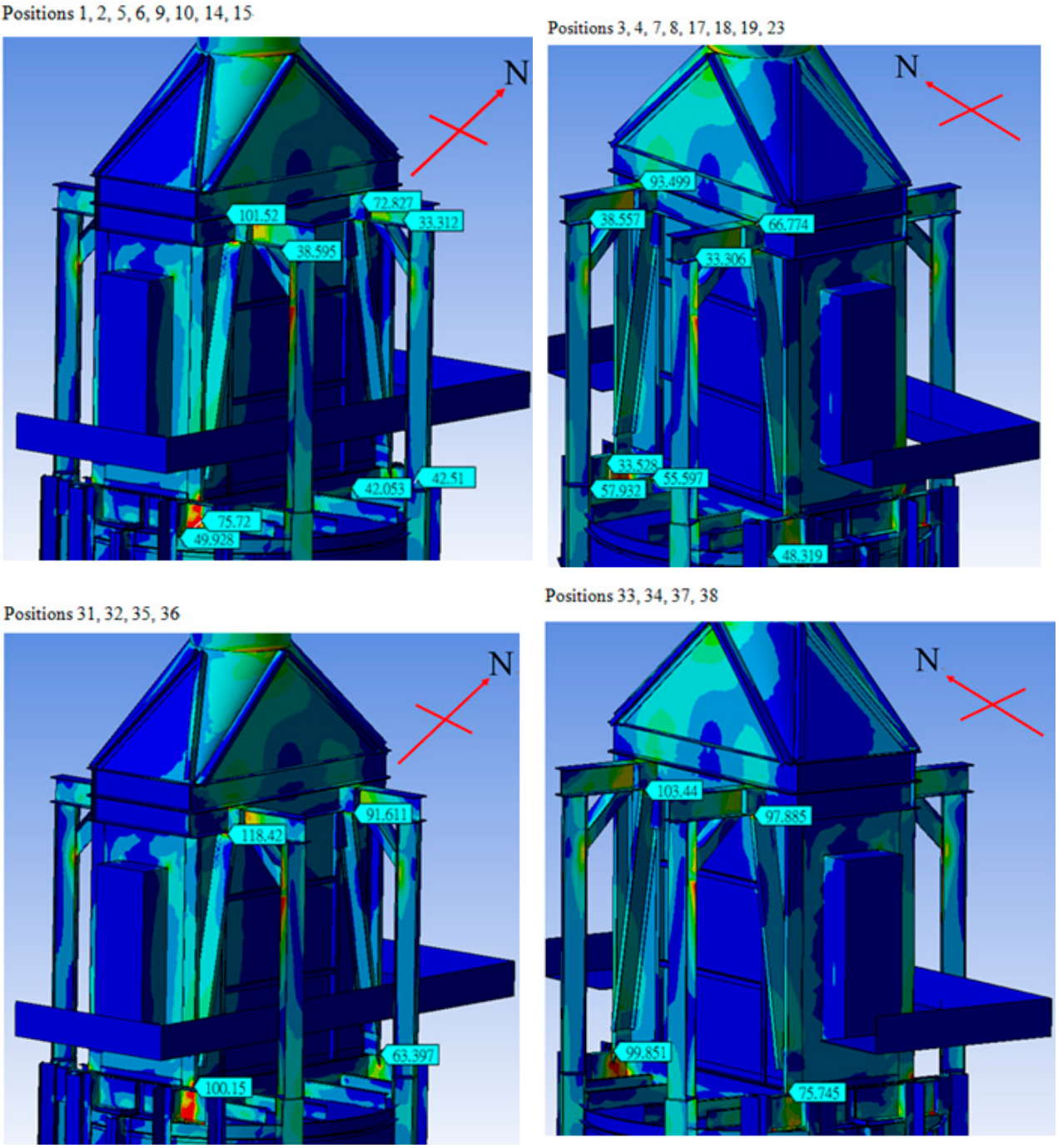

Figure 7. Results of finite element analysis for the present heater.

To further improve the security of the heater, eight different kinds of reinforcement methods for the support frame, as illustrated in Figure 8, were analyzed and compared. Case 1 and 2 were designed by adding one or two vertical cross-type braces to Figure 3c and were expected to be able to enhance the strength of the vertical beams. Further, Case 2 was expected to be more effective than Case 1. Case 3 and 4 were designed by adding horizontal cross-type braces to the horizontal beams on the top of convection sections of Case 1 and 2, respectively, and were expected to be able to enhance the strength of the horizontal beams. Case 5 and 6 were designed by adding vertical or horizontal-plus-vertical braces to the horizontal beams on the top of convection section of Case 3 and were expected to be able to enhance the strength of the horizontal beams. Further, Case 6 was expected to be more

effective than Case 5. Case 7 and 8 were designed by adding vertical or horizontal-plus-vertical braces to the horizontal beams on the top of convection section of Case 4 and were expected to be able to enhance the strength of the horizontal beams. Further, Case 8 was expected to be the most effective one among the eight cases investigated.

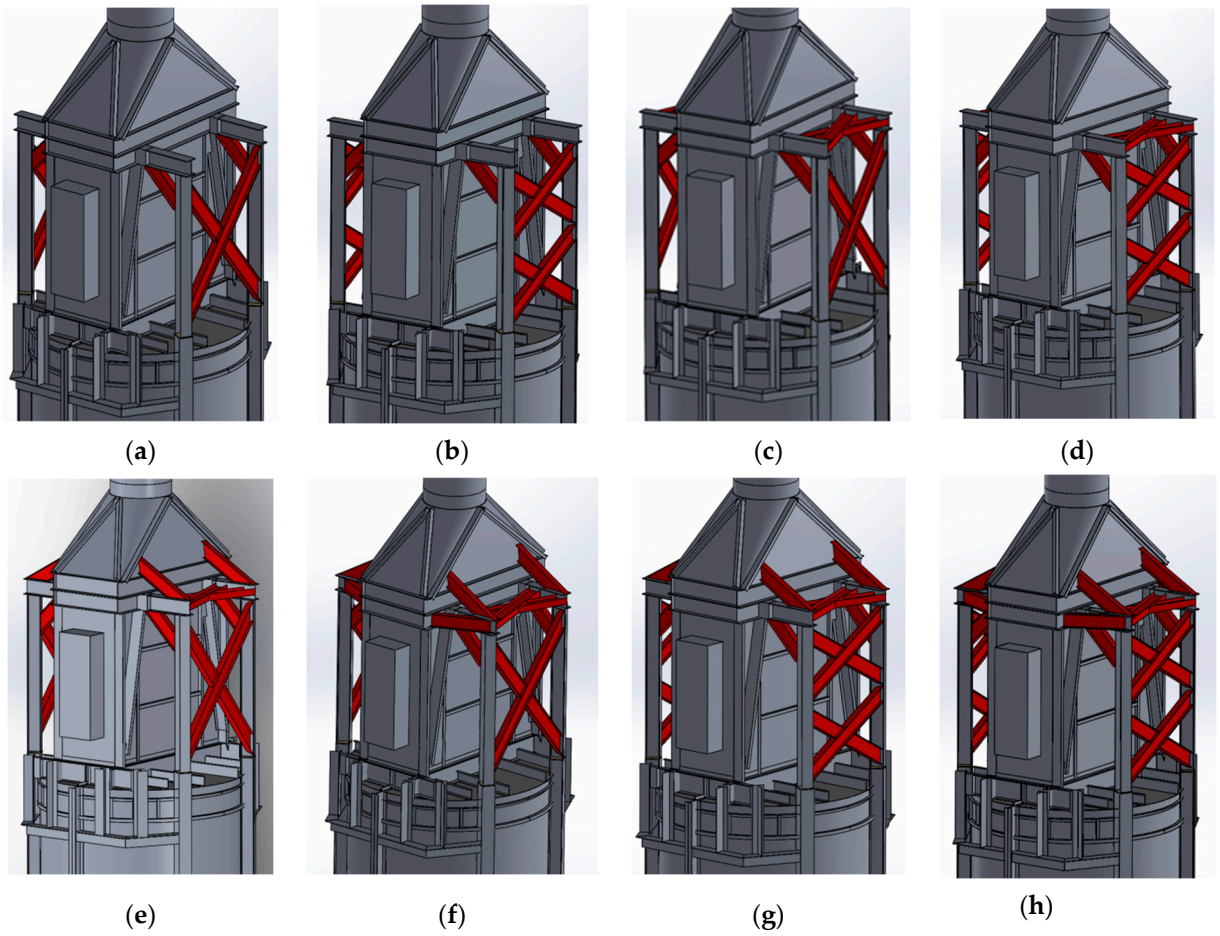

Figure 8. Eight different kinds of reinforcement methods for the support frame. (**a**) Case 1; (**b**) Case 2; (**c**) Case 3; (**d**) Case 4; (**e**) Case 5; (**f**) Case 6; (**g**) Case 7; (**h**) Case 8.

From the results of finite element analysis, the stresses at all positions for the eight cases shown in Figure 8 were lower than the fatigue limit. As expected, Case 8 was the most effective one among the eight cases investigated. However, positions 10, 18, 31, 34, 35, and 38 were still in potential threat because their stresses were close to the fatigue limit, as shown in Figure 9. When the wind speed increases, the stresses at the above-mentioned positions will exceed the fatigue limit. To further enhance the security of the heater, Case 9 was proposed by modifying Case 8, as illustrated in Figure 10. The four braces at the top of convection section for Case 8 were removed because one end of the brace was welded to the skin of the heater and this may be harmful to the skin under the action of a strong wind, as marked in Figure 10a. Further, four braces at the bottom of the convection section were added in Case 9 to share the forces acting on the bottom of the convection section, as indicated by the green marks in Figure 10b,c. The inclined angles of the four braces at the top of convection section for Case 9 were changed from 45° in Case 8 to 60° in Case 9 because this was more effective in reducing stresses after finite element analysis, as indicated by the yellow marks in Figure 10b,c.

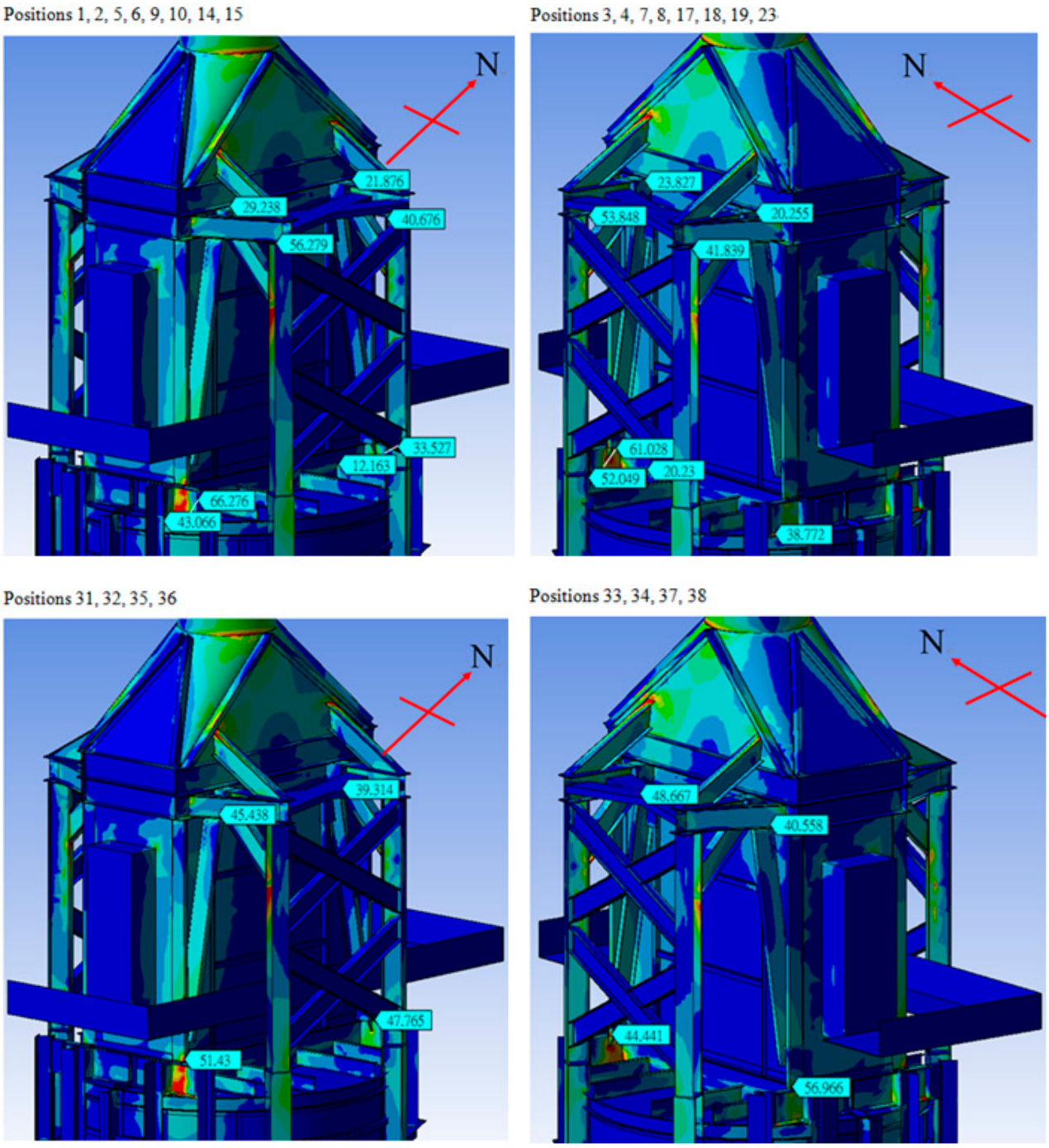

Figure 9. Results of finite element analysis for Case 8.

From the results of the finite element analysis for Case 9, as shown in Figure 11, the stresses at all positions were lower than the fatigue limit, and the stresses at positions 10, 18, 31, 34, 35, and 38 were further reduced, as compared to Case 8. The wind speed that the heater can withstand was also increased, as will be analyzed below. Because the stack bore most of the wind load, the wind flowing through a heater could be reasonably simplified as flow past a cylinder. Therefore, the relation between the wind speed and the stress could be derived from Schlichting's diagram of drag coefficient vs. Reynolds number [26], as shown in Figure 12.

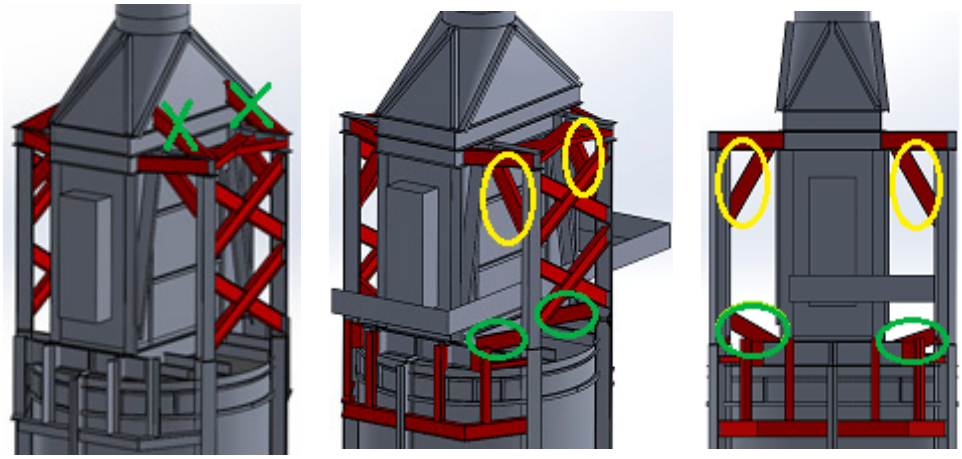

(**a**) (**b**) (**c**)

Figure 10. Numerical model for Case 9. (**a**) Case 8 (The braces with green marks are removed.); (**b**) Case 9 (The braces with green marks are added and the brace angles with yellow marks are changed, similar for (**c**)), (**c**) Case 9.

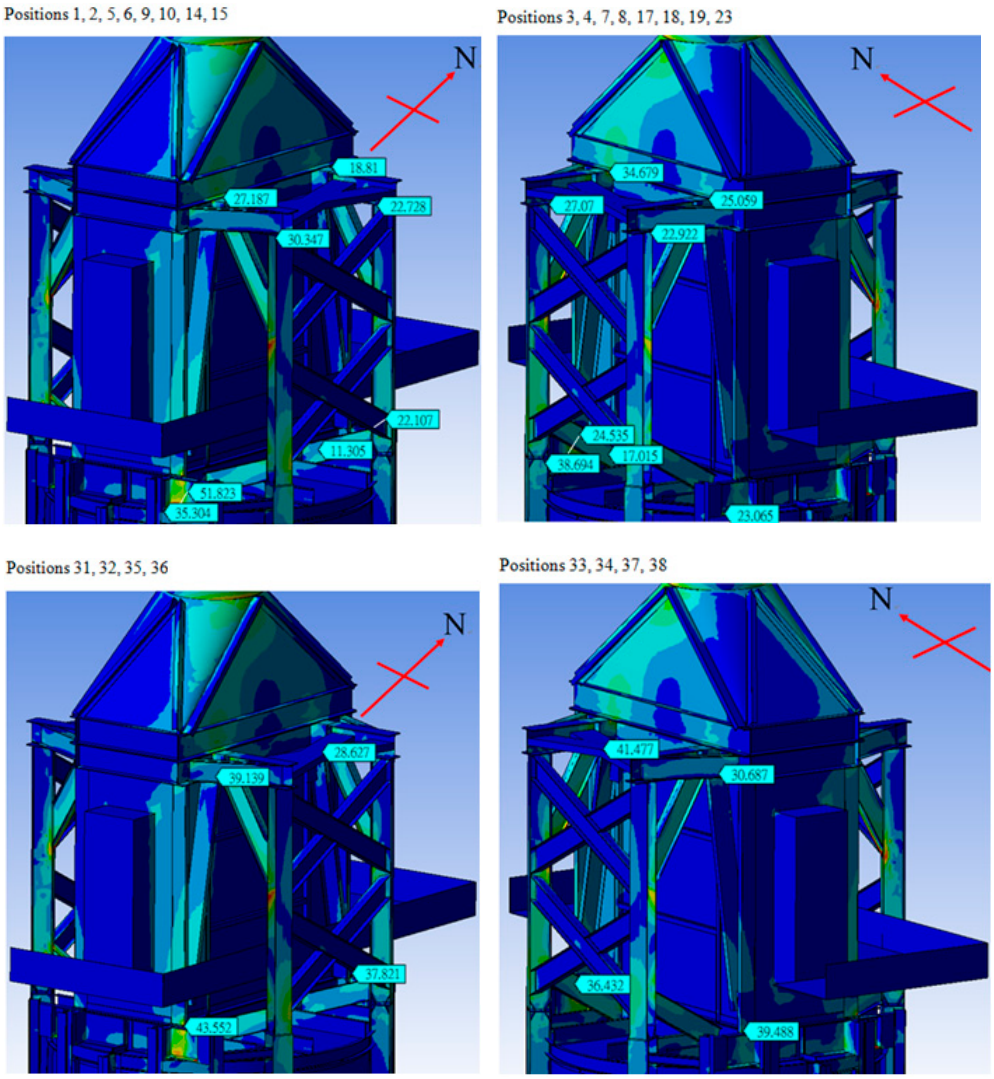

Figure 11. Results of finite element analysis for Case 9.

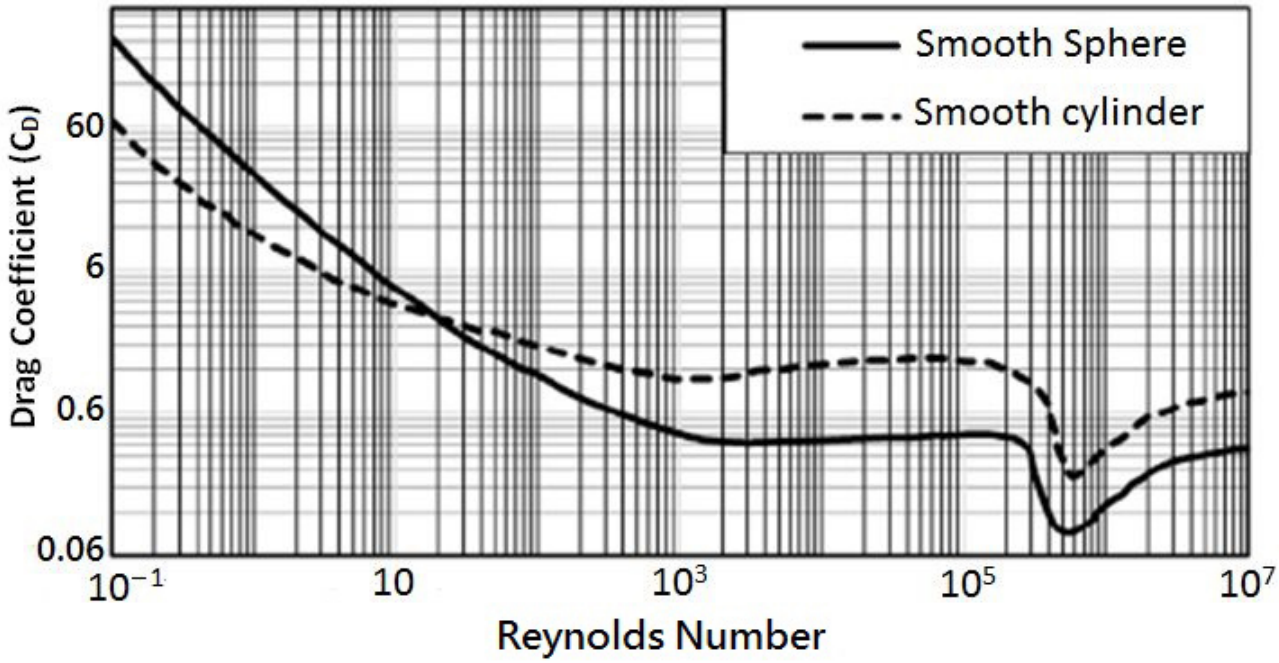

Figure 12. Drag coefficient of ideal sphere and circular cylinder by Schlichting.

The drag force for flow past a cylinder is written as:

$$F_D = C_D \times (1/2)\rho V^2 A \quad (1)$$

where C_D is the drag coefficient, ρ is the air density, V is the wind speed, and A is the frontal area of the stack. From Equation (1), the drag force F_D is proportional to $C_D \times V^2$. Because the stress (τ) is proportional to the drag force, it is also proportional to $C_D \times V^2$. The drag coefficient C_D can be found from Figure 8. The Reynolds number (Re) is computed from $Re = \rho VD/\mu$, where D is the stack diameter and μ is the air viscosity. The critical wind speed, V_c, when the stress of the support frame reaches the fatigue limit, τ_f, can then be solved from the following equation:

$$\tau_f/\tau_{ref} = (C_{D,c} \times V_c^2)/(C_{D,ref} \times V_{ref}^2) \quad (2)$$

where $C_{D,c}$ and $C_{D,ref}$ are the drag coefficients corresponding to the critical wind speed, V_c, and reference wind speed, V_{ref}, respectively. In this study, V_{ref} was taken as the maximum wind speed, 22 m/s, in the vibration monitoring period in Section 3 because its stress measurement data were available. For case 8, it was found from the solution of Equation (2) that the critical wind speed, V_c, was approximately 23 m/s. On the other hand, for case 9, it was found that the critical wind speed, V_c, was approximately 26 m/s. Case 9 clearly increased the wind speed that the heater could withstand and therefore improved its security. We then evaluated the fatigue life of the support frame from the S-N curve [27] for the material of the heater, as shown in Figure 13. Consider a strong wind speed of 35 m/s, which has been detected at the site of the heater. We desired the heater to be able to withstand the highest wind speed on record, and therefore 35 m/s was taken into account. This value is equivalent to the Beaufort scale of 12. The stresses of the heater at a wind speed of 35 m/s can be estimated from Equation (3).

$$\tau/\tau_{ref} = (C_D \times V^2)/(C_{D,ref} \times V_{ref}^2) \quad (3)$$

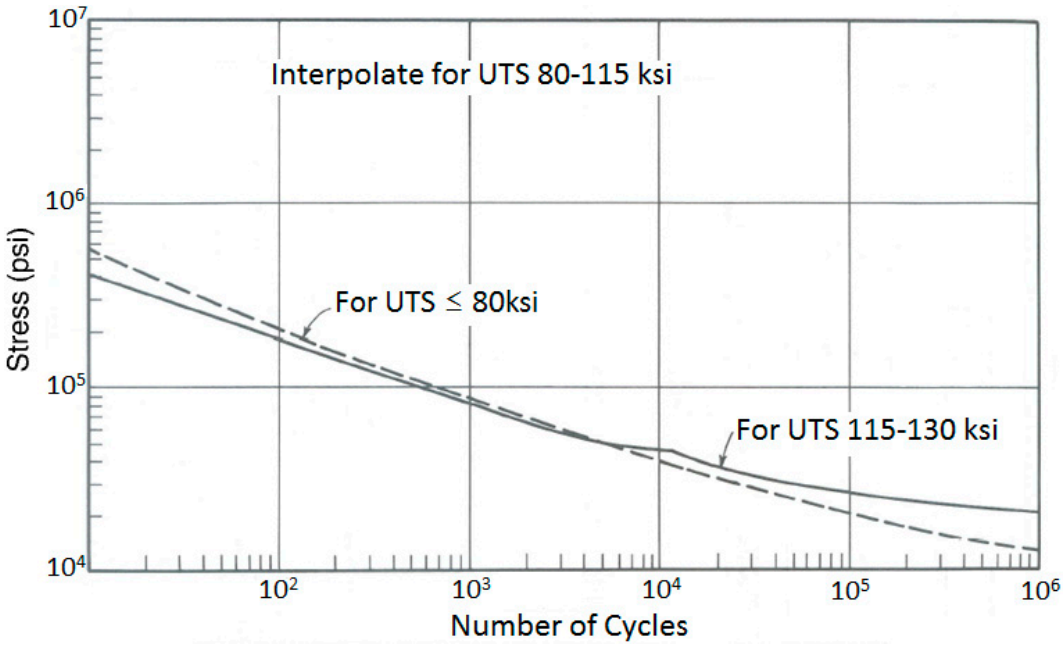

Figure 13. S–N curve for the material of the heater (ASTM A36, UTS = 58 ksi, or 400 MPa).

It was found that the fatigue life for cases 8 and 9 were 37,000 and 105,000 cycles, respectively, at a wind speed of 35 m/s. Case 9 could increase the fatigue life of the support frame by a factor of 183%.

5. Conclusions

5.1. Main Findings

In this paper, we investigated the operating security of a petrochemical heater under the action of a strong wind. In situ measurement and finite element analysis were carried out to analyze the stress distribution of the heater. We then proposed improvement suggestion for the support frame overhaul to ensure its operating security. From the results of the in situ measurement and finite element analysis, it was found that fatigue failure of the support frame before reinforcement occurred at locations where the computed stress by finite element method was large, thereby partially justifying the adequacies of our analysis methods and results. Among the nine reinforcement methods investigated, *Case 8 and Case 9 were superior to the other seven cases. Case 8 could withstand wind speeds up to 23 m/s, while Case 9 could withstand wind speeds up to 26 m/s.* Further, Case 9 could increase the fatigue life of the heater by a factor of 183%, as compared with Case 8. Therefore, among the nine different kinds of reinforcement methods investigated, we suggest adopting Case 9 to reinforce the support frame.

5.2. Future Work

We suggest verifying the performance of Case 9 during a northeast monsoon or typhoon. The locations where fatigue failure had occurred or were expected to occur through stress analysis are suggested as the positions to monitor. After finishing stress monitoring, we suggest establishing an automatic stress analyzing and monitoring system by at least one of two methods. The first method is to install an anemorumbometer on the stack to continuously monitor the wind speed and direction. When the wind speed exceeds the critical value predicted from the Schlichting's theory, a warning signal is issued. The second method is to install a strain gauge on the locations of large stresses detected in situ and then continuously monitor the stresses. When the monitored stress exceeds the fatigue limit, a warning signal is issued. The above two methods can be established simultaneously. When warning signals are issued by either of the two methods, the support frame is in a

dangerous operating status. Inspection should be performed thereafter to check the security of the support frame, and necessary repair and improvement tasks should be performed.

Funding: This research was funded by Formosa Petrochemical Corporation, Taiwan, under the contract 111-AF-016.

Institutional Review Board Statement: Not applicable.

Informed Consent Statement: Not applicable.

Data Availability Statement: The data presented in this study are available on request from the corresponding author.

Conflicts of Interest: The authors declare no conflict of interest.

References

1. Huang, W.; Gould, P.L.; Martinez, R.; Johnson, G.S. Dynamic response of a collapsed heater stack Metropolis and Beyond. In Proceedings of the 2005 Structures Congress and the 2005 Forensic Engineering Symposium, New York, NY, USA, 20–24 April 2005; pp. 1879–1889.
2. Haratian, M.; Amidpour, M.; Hamidi, A. Modeling and optimization of process fired heaters. *Appl. Therm. Eng.* **2019**, *157*, 113722. [CrossRef]
3. Guo, Y.; Cao, W.W.; Yan, P.; Qian, S.Y. Exploration and development of natural gas heaters with high fuel efficiency. *Nat. Gas Ind.* **2009**, *29*, 97–100. [CrossRef]
4. Rosli, M.N.; Aziz, N. Steady state modelling of steam cracking furnace radiant section using Aspen PLUS. *Mater. Today Proc.* **2018**, *5*, 21780–21789. [CrossRef]
5. Liu, F. Optimized Design of the High Temperature Furnace Heater Structure. Master's Thesis, Beijing University of Technology, Beijing, China, 2011. ProQuest Dissertations Publishing.
6. Jiang, Y.; Liu, T.; Bai, Y. Earthquake response analysis of tall reinforced concrete chimneys considering eccentricity. *Shock. Vib.* **2020**, *2020*, 1417969. [CrossRef]
7. Scarabino, A.; Bacchi, F. CFD analysis of a heater chimney with and without a flow straightener. In Proceedings of the 12th Americas Conference on Wind Engineering 2013, ACWE 2013: Wind Effects on Structures, Communities, and Energy Generation, Seattle, WA, USA, 16–20 June 2013; Volume 3, pp. 1373–1383.
8. Kolanu, N.R.; Raju, G.; Ramji, M. A unified numerical approach for the simulation of intra and inter laminar damage evolution in stiffened CFRP panels under compression. *Compos. Part B Eng.* **2020**, *190*, 107931. [CrossRef]
9. Armentani, E.; Caputo, F.; Esposito, L.; Giannella, V.; Citarella, R. Multibody Simulation for the Vibration Analysis of a Turbocharged Diesel Engine. *Appl. Sci.* **2018**, *8*, 1192. [CrossRef]
10. Armentani, E.; Giannella, V.; Citarella, R.; Parente, A.; Pirelli, M. Substructuring of a Petrol Engine: Dynamic Characterization and Experimental Validation. *Appl. Sci.* **2019**, *9*, 4969. [CrossRef]
11. Leta, J.V.; Dirham, T.R.; Dobis, J.; Guo, R.; Roberts, L. A probabilistic approach to fired heater tube remaining life assessments. In Proceedings of the ASME 2015 Pressure Vessels and Piping Conference (PVP2015), Boston, MA, USA, 19–23 July 2015. paper no. PVP2015-45427.
12. Swaminathan, J.; Guguloth, K.; Gunjan, M.; Roy, P.; Ghosh, R. Failure analysis and remaining life assessment of service exposed primary reformer heater tubes. *Eng. Fail. Anal.* **2008**, *15*, 311–331. [CrossRef]
13. Ray, A.K.; Sinha, S.K.; Tiwari, Y.N.; Swaminathan, J.; Das, G.; Chaudhuri, S.; Singh, R. Analysis of failed reformer tubes. *Eng. Fail. Anal.* **2003**, *10*, 351–362. [CrossRef]
14. Giannella, V. Stochastic approach to fatigue crack-growth simulation for a railway axle under input data variability. *Int. J. Fatigue* **2021**, *144*, 106044. [CrossRef]
15. Matta, L.M.; Szasz, G. Vibration and fatigue failures at pipeline facilities. In Proceedings of the 12th International Pipeline Conference, Calgary, AB, Canada, 24–28 September 2018.
16. Harper, C.B. AIV and FIV IN pipelines, plants, and facilities. In Proceedings of the 11th International Pipeline Conference, Calgary, AB, Canada, 26–30 September 2016.
17. Jansson, L.G.; Zeng, L.; Börjesson, A. On piping vibration and practical measures for preventing vibration-related damage. In Proceedings of the ASME 2016 Pressure Vessels and Piping Conference, Vancouver, BC, Canada, 17–21 July 2016.
18. Yeh, C.-L. Effect of burner operation on the catalyst tube lifetime of a steam methane reformer: A numerical study. *Appl. Sci.* **2020**, *11*, 231. [CrossRef]
19. Yeh, C.L.; Yang, T.C.; Lai, K.L.; Ke, C.Y. Numerical Study of the Effect of Furnace Geometry on the Catalyst Tube Lifetime of a Steam Methane Reformer. In Proceedings of the 2021 IEEE 3rd Eurasia Conference on IOT, Communication and Engineering (ECICE), Taiwan, China, 29–31 October 2021; ISBN 978-1-6654-4516-0.
20. Yeh, C.L.; Yang, T.C.; Lai, K.L.; Ke, C.Y. Analysis of Small Bore-Piping Vibration Phenomenon. In Proceedings of the 2021 IEEE 3rd Eurasia Conference on IOT, Communication and Engineering (ECICE), Taiwan, China, 29–31 October 2021; ISBN 978-1-6654-4516-0.

21. Dassault Systèmes SolidWorks Corporation, 175 Wyman Street, Waltham, MA 02451, USA. Available online: https://www.solidworks.com/support/resource-center (accessed on 15 April 2022).
22. ANSYS, Inc., Southpointe, 2600 Ansys Drive, Canonsburg, PA 15317, USA. Available online: https://www.ansys.com/products#t=ProductsTab&sort=relevancy&layout=card&f:@products=[Workbench] (accessed on 15 April 2022).
23. Thomson, W.T. *Theory of Vibration with Applications*, 3rd ed.; CBS Publishers & Distributors: New Delhi, India, 2002.
24. Fung, Y.C. *Foundation of Solid Mechanics*; Prentice Hall: Lebanon, IN, USA, 1985.
25. ANSYS Inc. *Theory Reference for the Mechanical APDL and Mechanical Applications*; Release 12.0; ANSYS Inc.: Canonsburg, PA, USA, 2009.
26. Schlichting, H. *Boundary Layer Theory*; McGraw Hill: New York, NY, USA, 1968.
27. The American Society of Mechanical Engineers. *Appendix 5 Mandatory Design Based on Fatigue Analysis, ASME Boiler & Pressure Vessel Code, Section VIII, Division 2*; The American Society of Mechanical Engineers: New York, NY, USA, 1995.